

DOI: 10.11779/CJGE201610015

考虑竖向荷载影响的大直径管桩水平振动响应解析解

栾鲁宝^{1, 2}, 丁选明^{*1}, 刘汉龙¹, 郑长杰¹

(1. 山地城镇建设与新技术教育部重点实验室(重庆大学), 重庆 400045; 2. 河海大学土木与交通学院, 江苏 南京 210098)

摘要: 建立了黏弹性地基中受轴力作用的现浇大直径管桩水平振动响应计算模型, 通过引入势函数对土体振动方程进行解耦, 结合桩土耦合条件求得了桩顶复阻抗解析表达式。将该解退化到不考虑竖向荷载的水平振动响应解与已有理论解对比, 验证了该解的合理性。通过算例分析, 研究了竖向荷载、激振频率和桩长对管桩桩顶水平复阻抗、桩身位移和内力的影响, 研究结果表明: 复阻抗实部和虚部在桩土系统固有频率处均发生共振; 竖向荷载使管桩位移和内力发生重分布, 竖向荷载为零时, 位移、弯矩和剪力最大值均出现于管桩中上部, 随着竖向荷载增大, 其最大值均出现于桩底; 桩身水平位移随频率变化而变化, 管桩中下部转角、弯矩和剪力受频率影响较大; 桩身中下部位移和内力受桩长影响大于桩身其他部分; 无桩芯土时桩顶水平位移和转角比桩芯土存在时大。

关键词: 竖向荷载; 水平动荷载; 管桩; 解析解; 振动响应

中图分类号: TU471 文献标识码: A 文章编号: 1000-4548(2016)10-1859-10

作者简介: 栾鲁宝(1989-), 男, 硕士研究生, 主要从事桩基动力学方面的研究。E-mail: luanlub@163.com。

Analytical solution of lateral dynamic response of a large diameter pipe pile considering influence of axial load

LUAN Lu-bao, DING Xuan-ming, LIU Han-long, ZHENG Chang-jie

(1. Laboratory of New Technology for Construction of Cities in Mountain Area (Chongqing University), Ministry of Education, Chongqing 400045, China; 2. College of Civil and Transportation Engineering, Hohai University, Nanjing 210098, China)

Abstract: The horizontal vibration model for a large diameter pipe pile subjected to axial load in viscoelastic soil is established. The potential functions are adopted to decouple the governing equations of the soil. Analytical solution of the impedance of the pipe pile is obtained based on the assumption of perfect contact between the pile and the soil. This analytical solution can be perfectly simplified to the horizontal vibration solution of pipe pile without axial load, which demonstrates the validity of the solution deduced in this study. Numerical examples are presented to analyze the influences of axial load, excitation frequencies, and pile lengths on the complex impedances, displacements and internal forces. The results show that the complex impedance resonates at the inherent frequency of the pile-soil system. The vertical loads cause the redistribution of the displacements and internal forces of the pipe pile. The maximum displacement, bending moment and shear stress are located at the upper part of the pile shaft when the vertical load is 0, however, they move to the pile bottom gradually with the increase of the vertical load. The horizontal displacement of the pipe pile varies with the frequency. The changes of rotation angle, bending moment and shear force are obvious at the lower part of the pile shaft. The influences of pile length on displacement and internal force at the middle and bottom parts of the pile are more significant than those in the other parts. The displacements located at the upper part of the pile shaft without inner soil are larger than those with inner soil.

Key words: axial load; horizontal dynamic load; pipe pile; analytical solution; vibration response

0 引言

桩基础在工程应用中经常会受到波浪荷载、地震荷载等水平荷载作用, 水平动荷载下桩土耦合振动问题在最近几十年里受到学者的广泛关注。Novak 等^[1-4]研究了均一各向同性土层中桩水平振动问题。Doyle 等^[5]研究了部分嵌入弹性地基中的桩基水平振动。Eisenberger 等^[6]研究了完全嵌入和部分嵌入弹性地基

中的桩基水平振动问题, 并对两者进行了比较。Gazetas 等^[7]基于分象限假定和平面应变模型分析了桩水平振动动力阻抗。然而以上分析均假定土为单相介质, 实际土是由多相介质构成的, 因此杨军等^[8]提

基金项目: 国家自然科学基金项目(51378177, 51622803, 51420105013)

收稿日期: 2015-06-12

*通讯作者 (E-mail: dxmhhu@163.com)

出了饱和土中桩基水平振动辐射阻尼简化算法。尚守平等^[9]研究了忽略流体惯性的饱和土中桩基水平振动动力响应分析。余俊等^[10]在前人的基础上, 考虑了流体惯性和土层沿深度的变化研究了端承桩在饱和土层中的水平简谐振动特性。实际工程中桩基往往受到竖向静载和水平动载的共同作用, 然而, 上述分析均是局限于水平荷载, 没有考虑竖向荷载对桩水平振动响应的影响。竖向荷载因桩身挠曲变形产生附加弯矩, 附加的桩身挠曲变形和弯矩不可忽略, 即所谓的 $P-\Delta$ 效应。

由于问题的复杂性, 探究竖向荷载对桩基水平振动响应的研究尚不足。Halabe 等^[11]首先研究了单桩在竖向静荷载作用下的水平振动问题, 提出竖向静荷载对桩基水平振动有不可忽视的影响。周绪红等^[12]研究了桩受轴力作用时水平动力阻抗及动力相互作用因子, 指出轴力对桩动力阻抗及动力相互作用因子均存在影响。Catal^[13-14]基于小变形理论和 Winkler 模型, 给出了在弯矩、轴力和剪力共同作用下桩基自由振动的偏微分方程。上述学者均是基于 Winkler 模型理论对桩基动力特性进行的研究, 然而 Winkler 模型不能真正地反映桩-土之间的耦合振动。Lu 等^[15]采用 Muki 虚拟桩法研究了桩顶竖向荷载对水平振动响应的影响。

随着岩土工程技术的快速发展, 一种现浇混凝土大直径管桩由于其施工工艺简便, 节省大量混凝土并有效提高桩基承载等特点在软土地基处理方面得到了广泛的应用^[16-18]。Ding 等^[19]和 Zheng 等^[20-21]分别研究了在竖向和横向动荷载作用下管桩动力响应问题。竖向静荷载对桩基水平振动响应有着不可忽略的影响, 因此考虑竖向静荷载作用下的管桩水平振动响应问题值得研究。本文推导了竖向静荷载作用下管桩水平振动响应频域解析解, 推导出了管桩水平动力复阻抗的解析表达式, 对管桩的工程应用具有一定的参考意义。

1 计算模型和基本假定

计算简图如 1 所示, 管桩顶受到水平动荷载 $H(t)$ 作用, 桩长为 L , 管桩横截面面积为 A_p , 密度为 ρ_p , 管桩弹性模量为 E_p , 截面惯性矩为 I_p , 管桩截面外半径为 r_1 , 内半径为 r_2 , P 为竖向静荷载, $f_1(z)$ 和 $f_2(z)$ 分别为水平振动时轴向单位长度桩周土和桩芯土的横向作用力。

本文在建立方程时采用如下假定: ①管桩采用线弹性 Euler 杆件模拟, 忽略其剪切变形及转动惯性, 只考虑弯曲变形; ②桩土体系为小变形振动, 桩土接触良好, 接触面不发生滑移; ③忽略桩身在水平动荷载下的竖向变形; ④桩底完全固定。

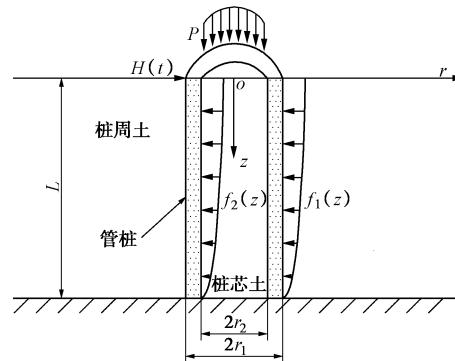


图 1 计算模型示意图

Fig. 1 Computational model

2 方程的建立

2.1 桩周土和桩芯土的振动方程

根据弹性动力学理论, 可以建立桩周土用位移表示的运动方程为

$$\left. \begin{aligned} &[(\lambda_1 + 2G_1) + i(\lambda'_1 + 2G'_1)] \frac{\partial e_1}{\partial r} - \frac{1}{r}(G_1 + iG'_1) \frac{\partial w_1}{\partial \theta} \\ &= -\rho_1 \omega^2 u_1 - (G_1 + iG'_1) \frac{\partial^2 u_1}{\partial z^2}, \\ &[(\lambda_1 + 2G_1) + i(\lambda'_1 + 2G'_1)] \frac{\partial e_1}{r \partial \theta} + (G_1 + iG'_1) \frac{\partial w_1}{\partial r} \\ &= -\rho_1 \omega^2 v_1 - (G_1 + iG'_1) \frac{\partial^2 v_1}{\partial z^2}. \end{aligned} \right\} \quad (1)$$

$$\left. \begin{aligned} e_1 &= \frac{\partial u_1}{\partial r} + \frac{u_1}{r} + \frac{1}{r} \frac{\partial v_1}{\partial \theta}, \\ w_1 &= \frac{\partial v_1}{\partial r} + \frac{v_1}{r} - \frac{1}{r} \frac{\partial u_1}{\partial \theta}. \end{aligned} \right\} \quad (2)$$

桩芯土用位移表示的运动方程为

$$\left. \begin{aligned} &[(\lambda_2 + 2G_2) + i(\lambda'_2 + 2G'_2)] \frac{\partial e_2}{\partial r} - \frac{1}{r}(G_2 + iG'_2) \frac{\partial w_2}{\partial \theta} \\ &= -\rho_2 \omega^2 u_2 - (G_2 + iG'_2) \frac{\partial^2 u_2}{\partial z^2}, \\ &[(\lambda_2 + 2G_2) + i(\lambda'_2 + 2G'_2)] \frac{\partial e_2}{r \partial \theta} + (G_2 + iG'_2) \frac{\partial w_2}{\partial r} \\ &= -\rho_2 \omega^2 v_2 - (G_2 + iG'_2) \frac{\partial^2 v_2}{\partial z^2}. \end{aligned} \right\} \quad (3)$$

式中 u_1 , v_1 和 u_2 , v_2 分别为桩周土和桩芯土的水平径向位移和环向位移; λ_1 , G_1 和 λ'_1 , G'_1 分别为桩周土复 Lame 常数的实部和虚部; λ_2 , G_2 和 λ'_2 , G'_2 分别为桩芯土复 Lame 常数的实部和虚部; ρ_1 , ρ_2 分别为桩周土和桩芯土的质量密度; ω 为激振频率。

2.2 管桩振动方程的建立

如图 2 所示, 取土体中管桩某一微元考虑, 其单位长度质量为 m , 两端作用有弯矩 $M(z, t)$, 剪力 $H(z, t)$ 和轴力 $A_p P$, 图中 α 为微元体偏转角度。

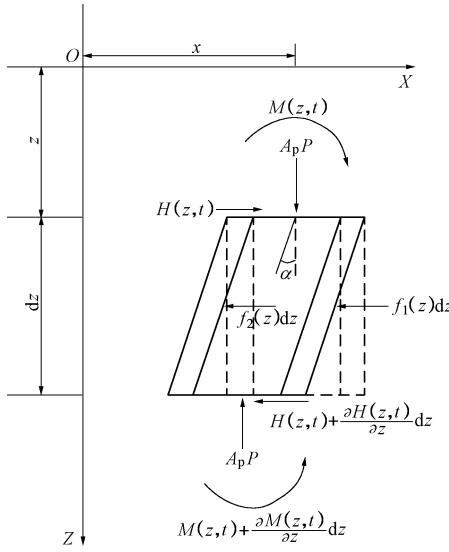


图2 微元体

Fig. 2 Element of volume

对图2中微元体下端中点取矩并略去二阶微分可得

$$H(z,t) - A_p P \frac{\partial u_p(z)}{\partial z} - \frac{\partial M(z,t)}{\partial z} = 0 , \quad (4)$$

由水平方向动力平衡方程可得

$$\frac{\partial H(z,t)}{\partial z} + m \frac{\partial u_p^2(z)}{\partial t^2} + f_1(z) + f_2(z) = 0 , \quad (5)$$

由材料力学中位移与弯矩关系可得

$$\frac{\partial u_p^2(z)}{\partial z^2} = \frac{M(z,t)}{E_p I_p} . \quad (6)$$

将式(6)对z求偏导可得

$$\frac{\partial u_p^3(z)}{\partial z^3} = \frac{\partial M(z,t)}{\partial z} . \quad (7)$$

将式(4)代入式(7)中并将所得式子对z求偏导可得

$$\frac{\partial u_p^4(z)}{\partial z^4} - \frac{1}{E_p I_p} \frac{\partial H(z,t)}{\partial z} + \frac{A_p P}{E_p I_p} \frac{\partial u_p^2(z)}{\partial z^2} = 0 . \quad (8)$$

将式(5)代入式(8)中可得

$$E_p I_p \frac{\partial^4 u_p(z)}{\partial z^4} + A_p P \frac{\partial^2 u_p(z)}{\partial z^2} + m \frac{\partial^2 u_p(z)}{\partial t^2} + f_1(z) + f_2(z) = 0 , \quad (9)$$

式中, $A_p P \frac{\partial^2 u_p(z)}{\partial z^2}$ 表示竖向荷载P对管桩水平振动的影响。

3 方程的求解

3.1 桩周土振动方程求解

引入势函数 $\varphi_1(r, \theta, z, t)$ 和 $\psi_1(r, \theta, z, t)$:

$$\left. \begin{aligned} u_1 &= \frac{\partial \varphi_1}{\partial r} + \frac{1}{r} \frac{\partial \psi_1}{\partial \theta} , \\ v_1 &= \frac{1}{r} \frac{\partial \varphi_1}{\partial \theta} - \frac{\partial \psi_1}{\partial r} . \end{aligned} \right\} \quad (10)$$

容易得到 $e_1 = \nabla^2 \varphi_1$, $w_1 = -\nabla^2 \psi_1$ 。将势函数代入式(1)中可得

$$[(\lambda_1 + 2G_1) + i(\lambda'_1 + 2G'_1)] \nabla^2 \varphi_1 + \left[\rho_1 \omega^2 + (G_1 + iG'_1) \frac{\partial^2}{\partial z^2} \right] \varphi_1 = 0 , \quad (11)$$

$$(G_1 + iG'_1) \nabla^2 \psi_1 + \left[\rho_1 \omega^2 + (G_1 + iG'_1) \frac{\partial^2}{\partial z^2} \right] \psi_1 = 0 , \quad (12)$$

$$\text{式中, } \nabla^2 = \frac{\partial^2}{\partial r^2} + \frac{1}{r} \frac{\partial}{\partial r} + \frac{1}{r^2} \frac{\partial^2}{\partial \theta^2} .$$

采用分离变量法求解式(11)、(12), 假设 $\varphi_1 = R_{11}(r)\Theta_{11}(\theta)Z_{11}(z)$, 式(11)可以分解为

$$\frac{1}{R_{11}} \frac{d^2 R_{11}}{dr^2} + \frac{1}{r} \frac{1}{R_{11}} \frac{dR_{11}}{dr} - \frac{1}{r^2} m_1^2 = q_{11}^2 , \quad (13)$$

$$\frac{1}{Z_{11}} \frac{d^2 Z_{11}}{dz^2} = -g_1^2 , \quad (14)$$

$$\frac{1}{\Theta_{11}} \frac{d^2 \Theta_{11}}{d\theta^2} = -m_1^2 , \quad (15)$$

$$\text{式中, } q_{11}^2 = \frac{(1+iD_{s1})g_1^2 v_{s1}^2 - \omega^2}{\eta_1^2 v_{s1}^2 + i[(\eta_1^2 - 2)D_{v1} + 2D_{s1}]v_{s1}^2} , \quad D_{s1} = G'_1/G_1 ,$$

$D_{v1} = \lambda'_1/\lambda_1$, $\eta_1 = \sqrt{[(\lambda_1 + 2G_1)/G_1]}$, v_{l1} 和 v_{s1} 分别为桩周土纵向波速和剪切波速, η_1 为桩周土波速比, D_{s1} 和 D_{v1} 为阻尼比。

式(13)~(15)的解为

$$R_{11} = A_{11} K_{m_1}(q_{11} r) + B_{11} I_{m_1}(q_{11} r) , \quad (16)$$

$$Z_{11} = C_{11} \sin(g_1 z) + D_{11} \cos(g_1 z) , \quad (17)$$

$$\Theta_{11} = E_{11} \sin(m_1 \theta) + F_{11} \cos(m_1 \theta) , \quad (18)$$

式中 $I_{m_1}()$ 和 $K_{m_1}()$ 分别为第一类和第二类 m_1 阶修正 Bessel 函数, A_{11} , B_{11} , C_{11} , D_{11} , E_{11} , F_{11} 为待定系数, 可由桩土边界条件和连续性条件确定。

桩周土边界条件可表示为

$$u_1(r, \theta, z)|_{r \rightarrow \infty} = v_1(r, \theta, z)|_{r \rightarrow \infty} = 0 , \quad (19)$$

$$\frac{\partial u_1(r, \theta, z)}{\partial z}|_{z=0} = 0 , \quad (20)$$

$$u_1(r, \theta, z)|_{z=L} = v_1(r, \theta, z)|_{z=L} = 0 . \quad (21)$$

桩周土与桩的连续性条件可表示为

$$u_1(r, \theta, z) = u_p(z) \cos \theta , \quad (22)$$

$$v_1(r, \theta, z) = -u_p(z) \sin \theta . \quad (23)$$

将式(16)~(18)代入边界条件及连续性条件可得

$$g_{1n} = \frac{(2n-1)\pi}{2L} \quad (n=1, 2, 3, \dots) , \quad B_{11} = C_{11} = E_{11} = 0 , \\ m_1 = 1 . \quad (24)$$

因此可以得到

$$\varphi_1 = \sum_{n=1}^{\infty} A_{1n} K_1(q_{11n} r) \cos(g_{11n} z) \cos \theta , \quad (25)$$

同理可以得到

$$\psi_1 = \sum_{n=1}^{\infty} A_{2n} K_1(q_{12n}r) \cos(g_{1n}z) \sin\theta , \quad (26)$$

$$\text{式中, } q_{12}^2 = \frac{(1+iD_{s1})g_1^2 v_{s1}^2 - \omega^2}{(1+iD_{s1})v_{s1}^2} .$$

因此桩周土径向和环向位移可以表示为

$$u_1(r, \theta, z) = \sum_{n=1}^{\infty} \left\{ A_{2n} \frac{K_1(q_{12n}r)}{r} - A_{1n} \cdot \left[\frac{K_1(q_{11n}r)}{r} + q_{11n} K_0(q_{11n}r) \right] \right\} \cos(g_{1n}z) \cos\theta . \quad (27)$$

$$v_1(r, \theta, z) = \sum_{n=1}^{\infty} \left\{ A_{2n} \left[\frac{K_1(q_{12n}r)}{r} + q_{12n} K_0(q_{12n}r) \right] - A_{1n} \frac{K_1(q_{11n}r)}{r} \right\} \cos(g_{1n}z) \sin\theta . \quad (28)$$

由桩周土与桩的连续性条件可得

$$A_{2n} = \gamma_{1n} A_{1n} , \quad (29)$$

$$\text{式中, } \gamma_{1n} = \frac{2K_1(q_{11n}r_1) + r_1 q_{11n} K_0(q_{11n}r_1)}{2K_1(q_{12n}r_1) + r_1 q_{12n} K_0(q_{12n}r_1)} .$$

综上, 桩周土在 $r=r_1$ 处径向位移可以为

$$u_1(r, \theta, z) \Big|_{r=r_1} = \sum_{n=1}^{\infty} \eta_{1n} A_{1n} \cos(g_{1n}z) \cos\theta . \quad (30)$$

$$\text{式中 } \eta_{1n} = - \left[\frac{1}{r_1} K_1(q_{11n}r_1) + q_{11n} K_0(q_{11n}r_1) \right] + \gamma_{1n} \frac{1}{r_1} .$$

$$K_1(q_{12n}r_1) .$$

桩周土水平动力阻抗为

$$f_1(z) = - \int_0^{2\pi} (\sigma_1 \cos\theta - \tau_1 \sin\theta) \Big|_{r=r_1} r_1 d\theta \\ = \pi r_1 G_1 \sum_{n=1}^{\infty} \xi_{1n} A_{1n} \cos(g_{1n}z) . \quad (31)$$

$$\text{式中, } \xi_{1n} = - \left\{ \eta_1^2 + i \left[\frac{2D_{s1}}{D_{v1}(\eta_1^2 - 2)} \right] \right\} q_{11n}^2 K_1(q_{11n}r_1) - (1 +$$

$$iD_{s1}) \gamma_{1n} q_{12n}^2 K_1(q_{12n}r_1) .$$

3.2 桩芯土振动方程求解

桩芯土边界条件可表示为

$$u_2(r, \theta, z) \Big|_{r=0} < \infty, \quad v_2(r, \theta, z) \Big|_{r=0} < \infty , \quad (32)$$

$$\frac{\partial u_2(r, \theta, z)}{\partial z} \Big|_{z=0} = 0 , \quad (33)$$

$$u_2(r, \theta, z) \Big|_{z=L} = v_2(r, \theta, z) \Big|_{z=L} = 0 . \quad (34)$$

桩芯土连续性条件可表示为

$$u_2(r, \theta, z) = u_p(z) \cos\theta , \quad (35)$$

$$v_2(r, \theta, z) = -u_p(z) \sin\theta . \quad (36)$$

桩芯土求解过程与桩周土求解过程相同, 可以得到桩芯土振动方程的解为

$$\varphi_2 = \sum_{n=1}^{\infty} B_{1n} I_1(q_{21n}r) \cos(g_{2n}z) \cos\theta , \quad (37)$$

$$\psi_2 = \sum_{n=1}^{\infty} B_{2n} I_1(q_{22n}r) \cos(g_{2n}z) \sin\theta , \quad (38)$$

$$u_2(r, \theta, z) = \sum_{n=1}^{\infty} \left\{ B_{1n} \left[q_{21n} I_0(q_{21n}r) - \frac{1}{r} I_1(q_{21n}r) \right] + B_{2n} \frac{1}{r} I_1(q_{22n}r) \right\} \cos(g_{2n}z) \cos\theta , \quad (39)$$

$$v_2(r, \theta, z) = \sum_{n=1}^{\infty} \left\{ -B_{1n} \frac{1}{r} I_1(q_{21n}r) + B_{2n} \left[\frac{1}{r} I_1(q_{22n}r) - q_{22n} I_0(q_{22n}r) \right] \right\} \cos(g_{2n}z) \sin\theta , \quad (40)$$

式中, $g_{2n} = \frac{(2n-1)\pi}{2L}$, ($n=1, 2, 3, \dots$), $q_{21}^2 = \frac{(1+iD_{s2})g_2^2 v_{s2}^2 - \omega^2}{\eta_2^2 v_{s2}^2 + i[(\eta_2^2 - 2)D_{v2} + 2D_{s2}]v_{s2}^2}$, $q_{22}^2 = \frac{(1+iD_{s2})g_2^2 v_{s2}^2 - \omega^2}{(1+iD_{s2})v_{s2}^2}$, $D_{s2} = G'_2 / G_2$, $D_{v2} = \lambda'_2 / \lambda_2$, $\eta_2 = \sqrt{[(\lambda_2 + 2G_2)/G_2]}$, v_{s2} 和 v_{s2} 分别为桩芯土纵向波速和剪切波速, η_2 为桩芯土波速比, D_{s2} 和 D_{v2} 为阻尼比。

由桩芯土连续性条件可得

$$B_{2n} = \gamma_{2n} B_{1n} , \quad (41)$$

$$\text{式中, } \gamma_{2n} = \frac{q_{21n} I_0(q_{21n}r_2) - \frac{2}{r_2} I_1(q_{21n}r_2)}{q_{22n} I_0(q_{22n}r_2) - \frac{2}{r_2} I_1(q_{22n}r_2)} .$$

桩芯土在 $r=r_2$ 处径向位移和水平动力阻抗分别为

$$u_2(r, \theta, z) \Big|_{r=r_2} = \sum_{n=1}^{\infty} \eta_{2n} B_{1n} \cos(g_{2n}z) \cos\theta , \quad (42)$$

$$f_2(z) = \int_0^{2\pi} (\sigma_2 \cos\theta - \tau_2 \sin\theta) \Big|_{r=r_2} r_2 d\theta \\ = \pi r_2 G_2 \sum_{n=1}^{\infty} \xi_{2n} B_{1n} \cos(g_{2n}z) . \quad (43)$$

式中,

$$\eta_{2n} = q_{21n} I_0(q_{21n}r_2) - \frac{1}{r_2} I_1(q_{21n}r_2) + \gamma_{2n} \frac{1}{r_2} I_1(q_{22n}r_2) , \quad \xi_{2n} = - \left\{ \eta_2^2 + i \left[2D_{s2} + D_{v2}(\eta_2^2 - 2) \right] \right\} q_{21n}^2 I_1(q_{21n}r_2) - (1+iD_{s2}) \cdot \gamma_{2n} q_{22n}^2 I_1(q_{22n}r_2) .$$

3.3 管桩振动方程求解

桩底边界条件可表示为

$$u_p(z) \Big|_{z=L} = 0 \quad (\text{位移}) , \quad (44)$$

$$\frac{\partial u_p(z)}{\partial z} \Big|_{z=L} = 0 \quad (\text{转角}) . \quad (45)$$

桩顶边界条件可表示为

$$\frac{\partial^2 u_p(z)}{\partial z^2} \Big|_{z=0} = 0 \quad (\text{弯矩}) , \quad (46)$$

$$\frac{\partial^3 u_p(z)}{\partial z^3} \Big|_{z=0} = \frac{1}{E_p I_p} \quad (\text{剪力}) . \quad (47)$$

对于简谐振动, 在竖向静荷载作用下管桩水平振动基本方程可以写为

$$E_p I_p \frac{d^4 u_p(z)}{dz^4} + A_p P \frac{\partial^2 u_p(z)}{\partial z^2} - m\omega^2 u_p(z) = -f_1(z) - f_2(z) . \quad (48)$$

将式(31)、(43)代入式(48)中可得

$$\begin{aligned} & \frac{d^4 u_p(z)}{dz^4} + \beta_1^4 \frac{\partial^2 u_p(z)}{\partial z^2} - \beta_2^4 u_p(z) = \\ & \frac{-\pi}{E_p I_p} \left[r_1 G_1 \sum_{n=1}^{\infty} \xi_{1n} A_{1n} \cos(g_{1n} z) + r_2 G_2 \sum_{n=1}^{\infty} \xi_{2n} B_{1n} \cos(g_{2n} z) \right] . \end{aligned} \quad (49)$$

$$\text{式中, } \beta_1^4 = \frac{A_p P}{E_p I_p}, \quad \beta_2^4 = \frac{m\omega^2}{E_p I_p} .$$

此四阶常微分方程的解为

$$\begin{aligned} u_p(z) = & C_1 \sin(\alpha_1 z) + \\ & C_2 \cos(\alpha_1 z) + C_3 \sinh(\alpha_2 z) + C_4 \cosh(\alpha_2 z) - \\ & \sum_{n=1}^{\infty} \zeta_{1n} A_{1n} \cos(g_{1n} z) - \sum_{n=1}^{\infty} \zeta_{2n} B_{1n} \cos(g_{2n} z) , \end{aligned} \quad (50)$$

$$\begin{aligned} \text{式中, } \zeta_{1n} = & \frac{\pi r_1 G_1 \xi_{1n}}{E_p I_p (g_{1n}^4 - \beta_1^4 g_{1n}^2 - \beta_2^4)}, \quad \zeta_{2n} = \pi r_2 G_2 \xi_{2n} / \\ & [E_p I_p (g_{2n}^4 - \beta_1^4 g_{2n}^2 - \beta_2^4)] , \quad \alpha_1 = \sqrt{\frac{-\beta_1^4 - \sqrt{\beta_1^8 + 4\beta_2^4}}{2}}, \\ \alpha_2 = & \sqrt{\frac{-\beta_1^4 + \sqrt{\beta_1^8 + 4\beta_2^4}}{2}}, \quad C_1, \quad C_2, \quad C_3, \quad C_4 \text{ 为待定} \\ \text{常数。} \end{aligned}$$

由桩土完全接触条件, 可得

$$\begin{aligned} \sum_{n=1}^{\infty} \eta_{1n} A_{1n} \cos(g_{1n} z) = & C_1 \sin(\alpha_1 z) + \\ & C_2 \cos(\alpha_1 z) + C_3 \sinh(\alpha_2 z) + C_4 \cosh(\alpha_2 z) - \\ & \sum_{n=1}^{\infty} \zeta_{1n} A_{1n} \cos(g_{1n} z) - \sum_{n=1}^{\infty} \zeta_{2n} B_{1n} \cos(g_{2n} z) . \end{aligned} \quad (51)$$

$$\begin{bmatrix} u_p(z) \\ \phi_p(z) \\ M_p(z) \\ \frac{Q_p(z)}{E_p I_p} \end{bmatrix} = \begin{bmatrix} \sin(\alpha_1 z) - \sum_{n=1}^{\infty} \kappa_{1n} \cos(g_n z) & \cos(\alpha_1 z) - \sum_{n=1}^{\infty} \kappa_{2n} \cos(g_n z) & \sinh(\alpha_2 z) - \sum_{n=1}^{\infty} \kappa_{3n} \cos(g_n z) & \cosh(\alpha_2 z) - \sum_{n=1}^{\infty} \kappa_{4n} \cos(g_n z) \\ \alpha_1 \cos(\alpha_1 z) + \sum_{n=1}^{\infty} \kappa_{1n} g_n \sin(g_n z) & -\alpha_1 \sin(\alpha_1 z) + \sum_{n=1}^{\infty} \kappa_{2n} g_n \sin(g_n z) & \alpha_2 \cosh(\alpha_2 z) + \sum_{n=1}^{\infty} \kappa_{3n} g_n \sin(g_n z) & \alpha_2 \sinh(\alpha_2 z) + \sum_{n=1}^{\infty} \kappa_{4n} g_n \sin(g_n z) \\ -\alpha_1^2 \sin(\alpha_1 z) + \sum_{n=1}^{\infty} \kappa_{1n} g_n^2 \cos(g_n z) & -\alpha_1^2 \cos(\alpha_1 z) + \sum_{n=1}^{\infty} \kappa_{2n} g_n^2 \cos(g_n z) & \alpha_2^2 \sinh(\alpha_2 z) + \sum_{n=1}^{\infty} \kappa_{3n} g_n^2 \cos(g_n z) & \alpha_2^2 \cosh(\alpha_2 z) + \sum_{n=1}^{\infty} \kappa_{4n} g_n^2 \cos(g_n z) \\ -\alpha_1^3 \cos(\alpha_1 z) - \sum_{n=1}^{\infty} \kappa_{1n} g_n^3 \sin(g_n z) & \alpha_1^3 \sin(\alpha_1 z) - \sum_{n=1}^{\infty} \kappa_{2n} g_n^3 \sin(g_n z) & \alpha_2^3 \cosh(\alpha_2 z) - \sum_{n=1}^{\infty} \kappa_{3n} g_n^3 \sin(g_n z) & \alpha_2^3 \sinh(\alpha_2 z) - \sum_{n=1}^{\infty} \kappa_{4n} g_n^3 \sin(g_n z) \end{bmatrix} \begin{bmatrix} C_1 \\ C_2 \\ C_3 \\ C_4 \end{bmatrix} . \quad (58)$$

将式(44)~(47)边界条件代入式(58)中可得

$$\begin{aligned} \sum_{n=1}^{\infty} \eta_{2n} B_{1n} \cos(g_{2n} z) = & C_1 \sin(\alpha_1 z) + \\ & C_2 \cos(\alpha_1 z) + C_3 \sinh(\alpha_2 z) + C_4 \cosh(\alpha_2 z) - \\ & \sum_{n=1}^{\infty} \zeta_{1n} A_{1n} \cos(g_{1n} z) - \sum_{n=1}^{\infty} \zeta_{2n} B_{1n} \cos(g_{2n} z) . \end{aligned} \quad (52)$$

令 $g_n = g_{1n} = g_{2n}$, 由此可得

$$B_{1n} = \frac{\eta_{1n} A_{1n}}{\eta_{2n}} . \quad (53)$$

由三角函数的正交性可得

$$\int_0^L \cos(g_n z) \cos(g_m z) dz = \begin{cases} \frac{L}{2} & (m=n) \\ 0 & (m \neq n) \end{cases} . \quad (54)$$

在式(52)两端同时乘以 $\cos(g_n z)$, 并在区间 $[0, L]$ 上积分, 可得

$$A_{1n} = \eta_{2n} \delta_n (N_1 C_1 + N_2 C_2 + N_3 C_3 + N_4 C_4) . \quad (55)$$

$$\begin{aligned} \text{式中, } \delta_n = & \frac{2}{(\eta_{1n} \eta_{2n} + \eta_{1n} \zeta_{2n} + \zeta_{1n} \eta_{2n}) L}, \quad N_1 = \\ & \int_0^H \sin(\alpha_1 z) \cos(g_n z) dz, \quad N_2 = \int_0^H \cos(\alpha_1 z) \cos(g_n z) dz, \\ & N_3 = \int_0^H \sinh(\alpha_2 z) \cos(g_n z) dz, \quad N_4 = \int_0^H \cosh(\alpha_2 z) \cos(g_n z) dz . \end{aligned}$$

将 A_{1n} 代入式(50)中可得

$$B_{1n} = \eta_{1n} \delta_n (N_1 C_1 + N_2 C_2 + N_3 C_3 + N_4 C_4) , \quad (56)$$

将 A_{1n} , B_{1n} 代入式(50)中可得

$$\begin{aligned} u_p(z) = & C_1 \left[\sin(\alpha_1 z) - \sum_{n=1}^{\infty} \kappa_{1n} \cos(g_n z) \right] + \\ & C_2 \left[\cos(\alpha_1 z) - \sum_{n=1}^{\infty} \kappa_{2n} \cos(g_n z) \right] + \\ & C_3 \left[\sinh(\alpha_2 z) - \sum_{n=1}^{\infty} \kappa_{3n} \cos(g_n z) \right] + \\ & C_4 \left[\cosh(\alpha_2 z) - \sum_{n=1}^{\infty} \kappa_{4n} \cos(g_n z) \right] . \end{aligned} \quad (57)$$

$$\begin{aligned} \text{式中, } \kappa_{1n} = & (\eta_{1n} \zeta_{2n} + \zeta_{1n} \eta_{2n}) \delta_n N_1, \quad \kappa_{2n} = (\eta_{1n} \zeta_{2n} + \zeta_{1n} \eta_{2n}) \\ & \delta_n N_2, \quad \kappa_{3n} = (\eta_{1n} \zeta_{2n} + \zeta_{1n} \eta_{2n}) \delta_n N_3, \quad \kappa_{4n} = (\eta_{1n} \zeta_{2n} + \\ & \zeta_{1n} \eta_{2n}) \delta_n N_4 . \end{aligned}$$

由材料力学位移、转角、弯矩和剪力之间的关系可知:

$$\begin{bmatrix} 0 \\ 0 \\ 0 \\ \frac{1}{E_p I_p} \end{bmatrix} = \begin{bmatrix} \sin(\alpha_1 L) - \sum_{n=1}^{\infty} \kappa_{1n} \cos(g_n L) & \cos(\alpha_1 L) - \sum_{n=1}^{\infty} \kappa_{2n} \cos(g_n L) & \sinh(\alpha_2 L) - \sum_{n=1}^{\infty} \kappa_{3n} \cos(g_n L) & \cosh(\alpha_2 L) - \sum_{n=1}^{\infty} \kappa_{4n} \cos(g_n L) \\ \alpha_1 \cos(\alpha_1 L) + \sum_{n=1}^{\infty} \kappa_{1n} g_n \sin(g_n L) & -\alpha_1 \sin(\alpha_1 L) + \sum_{n=1}^{\infty} \kappa_{2n} g_n \sin(g_n L) & \alpha_2 \cosh(\alpha_2 L) + \sum_{n=1}^{\infty} \kappa_{3n} g_n \sin(g_n L) & \alpha_2 \sinh(\alpha_2 L) + \sum_{n=1}^{\infty} \kappa_{4n} g_n \sin(g_n L) \\ \sum_{n=1}^{\infty} \kappa_{1n} g_n^2 & -\alpha_1^2 + \sum_{n=1}^{\infty} \kappa_{2n} g_n^2 & \sum_{n=1}^{\infty} \kappa_{3n} g_n^2 & \alpha_2^2 + \sum_{n=1}^{\infty} \kappa_{4n} g_n^2 \\ -\alpha_1^3 & 0 & \alpha_2^3 & 0 \end{bmatrix} \begin{bmatrix} C_1 \\ C_2 \\ C_3 \\ C_4 \end{bmatrix}. \quad (59)$$

解式(59)可得

$$C_1 = \frac{(b_9 b_{11} - b_6 b_{12})(b_2 b_6 - b_3 b_5) - (b_3 b_{11} - b_6 b_{10})(b_6 b_8 - b_5 b_9)}{E_p I_p \gamma}, \quad (60)$$

$$C_2 = \frac{b_9 b_{11} - b_6 b_{12}}{E_p I_p (b_6 b_8 - b_5 b_9)} - \frac{b_6 b_7 - b_4 b_9}{b_6 b_8 - b_5 b_9} C_1, \quad (61)$$

$$C_3 = \frac{1}{E_p I_p \alpha_2^3} + \frac{\alpha_1^3}{\alpha_2^3} C_1. \quad (62)$$

$$C_4 = -\frac{b_{10}}{E_p I_p b_3} - \frac{b_1}{b_3} C_1 - \frac{b_2}{b_3} C_2. \quad (63)$$

式中, $b_1 = \alpha_2^3 \sin(\alpha_1 L) + \alpha_1^3 \sinh(\alpha_2 L)$, $b_2 = \alpha_2^3 \cos(\alpha_1 L)$, $b_3 = \alpha_2^3 \cosh(\alpha_2 L)$, $b_4 = \alpha_2^3 [\alpha_1 \cos(\alpha_1 L) + \sum_{n=1}^{\infty} \kappa_{1n} h_n \cdot \sin(h_n L)] + \alpha_1^3 [\alpha_2 \cosh(\alpha_2 L) + \sum_{n=1}^{\infty} \kappa_{3n} h_n \sin(h_n L)]$, $b_5 = \alpha_2^3 [-\alpha_1 \sin(\alpha_1 L) + \sum_{n=1}^{\infty} \kappa_{2n} h_n \sin(h_n L)]$, $b_6 = \alpha_2^3 [\alpha_2 \sinh(\alpha_2 L) + \sum_{n=1}^{\infty} \kappa_{4n} h_n \sin(h_n L)]$, $b_7 = \alpha_2^3 \sum_{n=1}^{\infty} \kappa_{1n} h_n^2 + \alpha_1^3 \sum_{n=1}^{\infty} \kappa_{3n} h_n^2$, $b_8 = \alpha_2^3 \left(\sum_{n=1}^{\infty} \kappa_{2n} h_n^2 - \alpha_1^2 \right)$, $b_9 = \alpha_2^3 \left(\sum_{n=1}^{\infty} \kappa_{4n} h_n^2 + \alpha_2^2 \right)$, $b_{10} = \sinh(\alpha_2 L)$, $b_{11} = \alpha_2 \cosh(\alpha_2 L) + \sum_{n=1}^{\infty} \kappa_{3n} h_n \sin(h_n L)$, $b_{12} = \sum_{n=1}^{\infty} \kappa_{3n} h_n$, $\gamma = (b_6 b_7 - b_4 b_9)(b_2 b_6 - b_3 b_5) - (b_1 b_6 - b_3 b_4)(b_6 b_8 - b_5 b_9)$ 。

至此, 待定系数全部确定。由桩顶动刚度的定义, 可得管桩桩顶水平动刚度 K_h 为

$$K_h = \frac{1}{-\sum_{n=1}^{\infty} \kappa_{1n} C_1 + \left(1 - \sum_{n=1}^{\infty} \kappa_{2n}\right) C_2 - \sum_{n=1}^{\infty} \kappa_{3n} C_3 + \left(1 - \sum_{n=1}^{\infty} \kappa_{4n}\right) C_4}. \quad (64)$$

管桩桩顶水平动力复阻抗可以表示为其实部和虚部的无量纲形式:

$$k_h = \frac{\operatorname{Re}(K_h) r_1^3}{E_p I_p}, \quad (65)$$

$$c_h = \frac{\operatorname{Im}(K_h) r_1^3}{E_p I_p}, \quad (66)$$

式中, $\operatorname{Re}()$ 表示实部, $\operatorname{Im}()$ 表示虚部。

4 管桩水平动力复阻抗特性分析

本文采取的计算参数如下: $L = 10 \text{ m}$, $r_1 = 0.5 \text{ m}$, $r_2 = 0.38 \text{ m}$, $\rho_p = 2.5 \text{ g/cm}^3$, $\rho_s = 2.0 \text{ g/cm}^3$, $E_p = 25 \text{ GPa}$, $\nu_1 = \nu_2 = 0.3$, $G_1 = G_2 = 10 \text{ MPa}$, $D_{s1} = D_{s2} = D_{v1} = D_{v2} = 0.02$ 。

4.1 合理性验证

为了验证本文解的合理性, 将本文解与文献[21]的水平振动响应解进行对比。

令 $P = 0$, 即退化到文献[21]水平振动响应解, 图 3 表明本文解与文献[21]解得到的结果吻合很好。由图 3 可以看出, 刚度部分最小处为桩土共振频率, 在共振频率以上, 实部随频率增大, 虚部随频率减小。

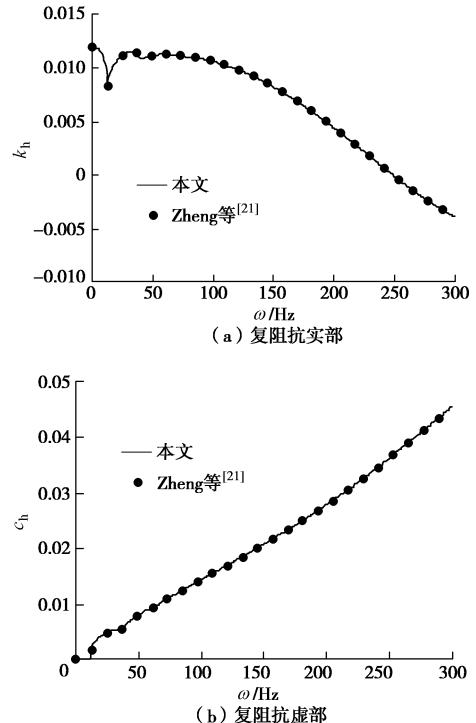


图 3 本文解与文献[21]解对比

Fig. 3 Comparison between author's and Zheng's solutions

4.2 坚向荷载对管桩水平振动复阻抗特性影响分析

图 4 给出了 500 Hz 频率范围内坚向荷载对管桩顶水平动力复阻抗的影响。复阻抗虚部突然增大的频率 ($\omega = 13 \text{ Hz}$) 为桩土系统固有频率, 复阻抗实部和虚部在桩土系统固有频率处发生共振, 复阻抗实部随频率增大而减小, 复阻抗虚部随频率增大而增大。从

图中可以看出, 在竖向荷载作用下, 复阻抗实部和虚部在 22 Hz 左右时会突然降低至最小值后增大, 且竖向荷载越大, 降低幅值越大; 竖向荷载对桩土系统共振频率和振荡幅值影响很小。

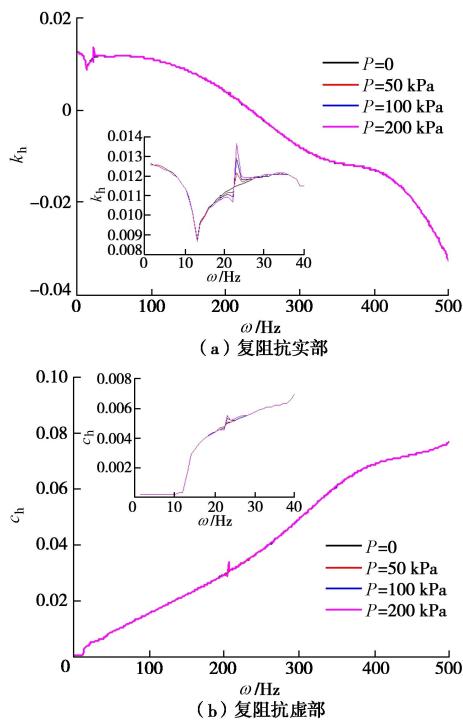


图 4 竖向荷载对管桩桩顶水平动力复阻抗的影响

Fig. 4 Variation of horizontal complex impedance with vertical loads

4.3 竖向荷载对管桩位移分布规律的影响

图 5, 6 给出了 $\omega = 22$ Hz 时竖向荷载对管桩水平位移和转角分布规律的影响。从图中可以看出, 竖向荷载会使管桩位移发生重分布; 桩顶没有竖向荷载作用时, 水平位移最大值和转角最大值均出现在桩顶, 水平位移和转角随深度先减小至 0 后反向增大, 最后减小至 0; 桩顶作用竖向荷载时, 桩身中下部水平位移和转角均随着竖向荷载增大而明显增大, 且增幅大于桩顶。

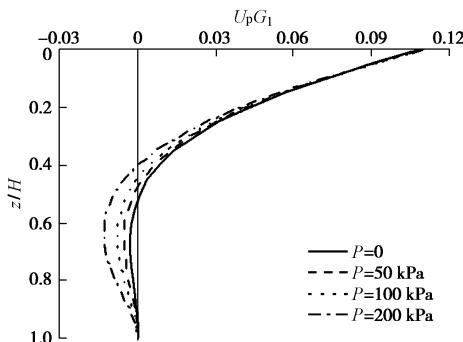


图 5 竖向荷载对管桩水平位移分布规律影响

Fig. 5 Variation of lateral displacement with different vertical loads

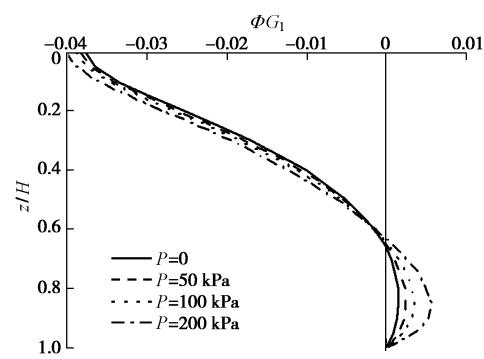


图 6 竖向荷载对管桩转角分布规律影响

Fig. 6 Variation of rotation angle with different vertical loads

4.4 竖向荷载对管桩内力分布规律的影响

图 7, 8 给出了 $\omega = 22$ Hz 时竖向荷载对管桩内力分布规律的影响。从图中可以看出, 竖向荷载会使管桩内力发生重分布; 桩顶没有竖向荷载作用时, 弯矩最大值和剪力最大值均集中于桩身中上部, 弯矩随深度的增加先增加后衰减至 0 最后反向增加, 剪力随深度增加迅速衰减至 0 后先反向增加后减小; 桩顶作用竖向荷载时, 桩身中下部弯矩和剪力均随着竖向荷载增大而明显增大, 且增幅大于桩身其他部分。

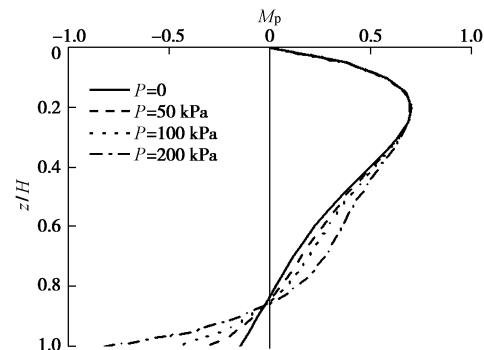


图 7 竖向荷载对管桩弯矩分布规律影响

Fig. 7 Variation of bending moment with different vertical loads

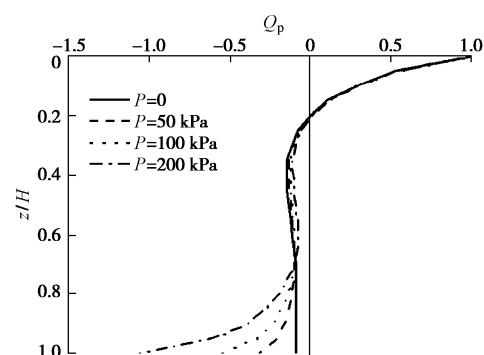


图 8 竖向荷载对管桩剪力分布规律影响

Fig. 8 Variation of shear force with different vertical loads

4.5 激振频率对管桩位移分布规律的影响

图 9, 10 给出了 $P = 100$ kPa 时桩土系统固有频率

(13 Hz)、竖向荷载作用下刚度突然降低的频率(22 Hz)和一般频率(30 Hz)对管桩位移分布规律的影响。由图可见,水平位移最大值和转角最大值出现在桩顶;水平位移和转角随深度先减小至0后反向增大,最后减小至0;桩身位移受频率影响较大,管桩中下部转角受频率影响较大。

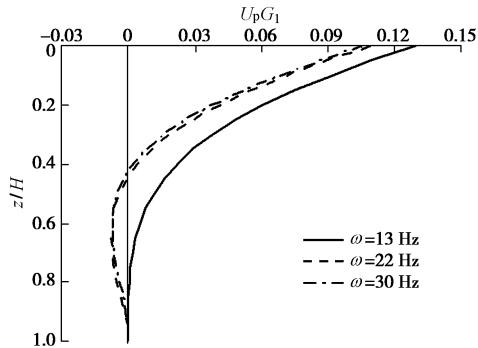


图 9 激振频率对管桩水平位移分布规律影响

Fig. 9 Variation of lateral displacement with different frequencies

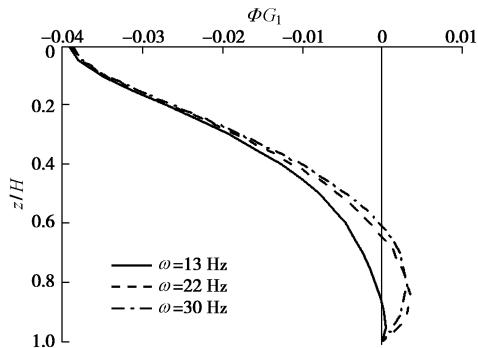


图 10 激振频率对管桩转角分布规律影响

Fig. 10 Variation of rotation angle with different frequencies

4.6 激振频率对管桩内力分布规律的影响

图 11, 12 给出了 $P = 100 \text{ kPa}$ 时桩土系统固有频率(13 Hz)、竖向荷载作用下刚度突然降低的频率(22 Hz)和一般频率(30 Hz)对管桩内力分布规律的影响。由图可见,反弯点位置随频率增大向桩顶移动;弯矩最大值出现在桩中上部,剪力最大值出现在桩顶;管桩中下部弯矩和剪力受频率影响较大。

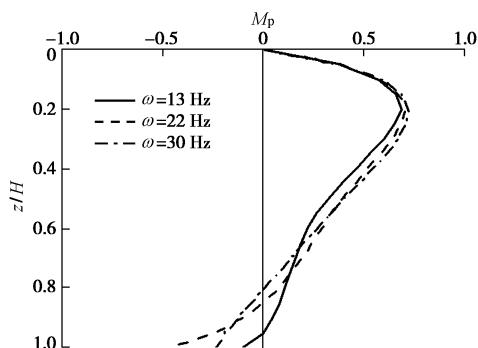


图 11 激振频率对管桩弯矩分布规律影响

Fig. 11 Variation of bending moment with different frequencies

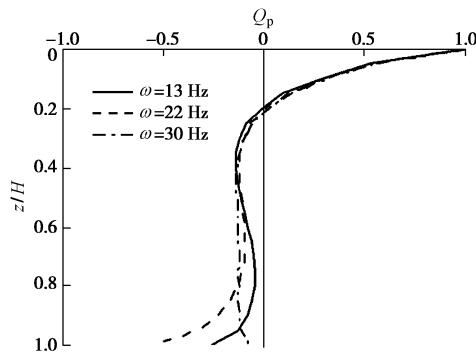


图 12 激振频率对管桩剪力分布规律影响

Fig. 12 Variation of shear force with different frequencies

4.7 桩长对管桩位移分布规律的影响

图 13, 14 给出了 $\omega = 22 \text{ Hz}$, $P = 100 \text{ kPa}$ 时桩长对管桩水平位移和转角分布规律的影响。从图中可以看出,4 种桩长的水平位移和转角分布规律类似,水平位移最大值和转角最大值均出现在桩顶;桩长取 10, 15 m 时,水平位移曲线和转角曲线均出现一次反向弯曲,桩长取 20, 25 m 时,水平位移曲线和转角曲线均出现两次反向弯曲;桩长对水平位移和转角分布规律的影响主要体现在桩身中下部。

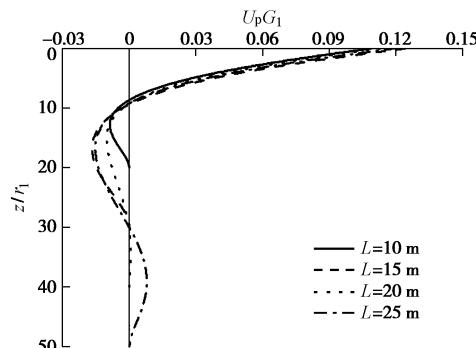


图 13 桩长对管桩水平位移分布规律影响

Fig. 13 Variation of lateral displacement with different pile lengths

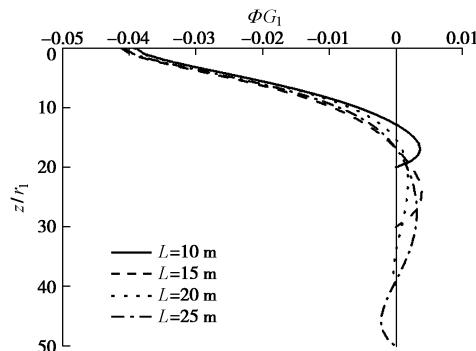


图 14 桩长对管桩转角分布规律影响

Fig. 14 Variation of rotation angle with different pile lengths

4.8 桩长对管桩内力分布规律的影响

图 15, 16 给出了 $\omega = 22 \text{ Hz}$, $P = 100 \text{ kPa}$ 时桩长对管桩弯矩和剪力分布规律的影响。从图中可以看出,4 种桩长的弯矩最大值均出现在桩身上部,剪力最大值均出现在桩顶;桩长取 10, 15 m 时,弯矩曲线和剪力曲线均出现一次反向弯曲,桩长取 20, 25 m 时,弯

矩曲线和剪力曲线均出现两次反向弯曲; 桩长对桩身弯矩和剪力分布规律的影响主要体现在桩身中下部。

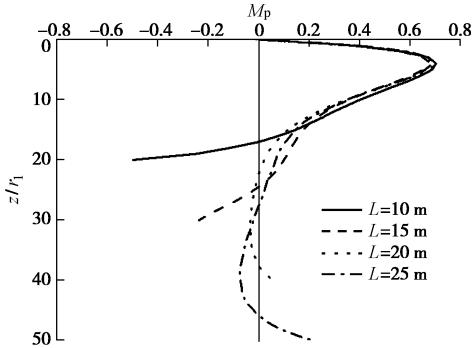


图 15 桩长对管桩弯矩分布规律影响

Fig. 15 Variation of bending moment with different pile lengths

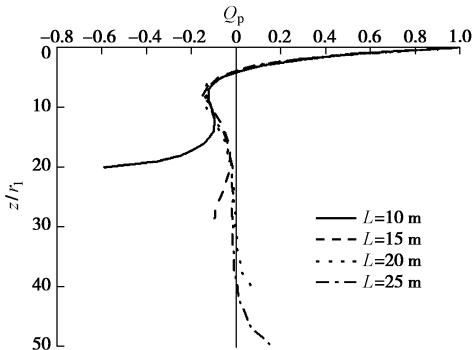


图 16 桩长对管桩剪力分布规律影响

Fig. 16 Variation of shear force with different pile lengths

4.9 桩芯土对管桩位移分布规律的影响

文献[21]研究表明, 在高频部分, 桩芯土对管桩水平振动有显著影响, 为了研究桩芯土存在与否对管桩位移的影响, 本文取 $\omega = 150 \text{ Hz}$ 。

图 17, 18 给出了 $\omega = 150 \text{ Hz}$, $P = 100 \text{ kPa}$ 时桩芯土存在与否对管桩水平位移和转角的影响。从图中可以看出, 无桩芯土时的桩顶水平位移幅值和转角幅值均明显大于有桩芯土时的桩顶水平位移和转角, 说明桩芯土对大直径管桩水平振动有显著影响。这是因为土体阻尼的存在, 桩芯土对振动有衰减的作用, 因此桩芯土存在时, 桩顶水平位移幅值和转角幅值均减小, 抗震效果有所提高。

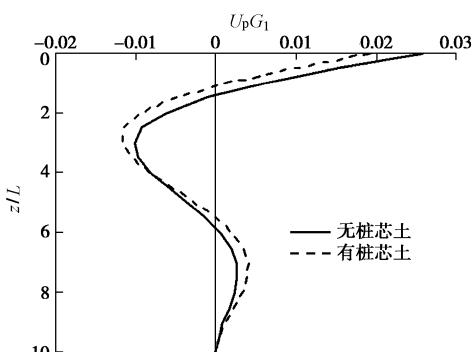


图 17 桩芯土对管桩水平位移分布规律影响

Fig. 17 Variation of lateral displacement with inner soil

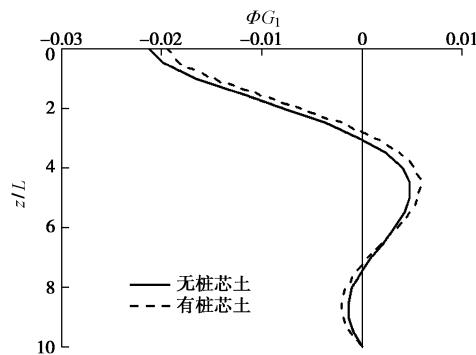


图 18 桩长对管桩转角分布规律影响

Fig. 18 Variation of rotation angle with inner soil

5 对工程的影响

(1) 实际工程中, 水平荷载使桩身产生较大的弯矩和挠曲变形, 坚向荷载对水平荷载产生的弯矩和挠曲变形有影响, 因此桩基水平承载力设计计算应该考虑坚向荷载的影响。

(2) 对弯矩的影响效应。对于桩顶承受相同水平荷载的管桩而言, 没有坚向荷载作用时, 弯矩最大值出现在桩身中上部, 受到坚向荷载作用后, 弯矩最大值有向桩底转移的趋势; 对于不同长度的管桩, 在坚向荷载作用下, 桩基会出现反向挠曲的现象。因此, 在实际工程配筋时要考虑最大弯矩在桩身的位置以及桩身的拉压状态, 以保证工程安全及提高材料利用率。

(3) 对位移的影响效应。对于桩顶承受相同水平荷载的管桩而言, 没有坚向荷载作用时, 水平位移最大值出现在桩顶, 受到坚向荷载作用后, 桩身中下部水平位移受坚向荷载影响明显; 对于不同桩长的管桩, 在坚向荷载作用下, 桩身中下部发生反向挠曲。因此, 在实际工程水平位移设计计算时应考虑坚向荷载及管桩桩长的影响。

6 结 论

(1) 管桩桩顶复阻抗实部和虚部在桩土系统固有频率处均发生共振, 震荡幅值随频率增大。

(2) 坚向荷载导致管桩复阻抗实部和虚部在频率 22 Hz 左右时突然降低至最小值后增大, 且坚向荷载越大, 降低幅值越大。

(3) 坚向荷载使管桩桩身水平位移和转角发生重分布, 坚向荷载为零时, 水平位移最大值和转角最大值均出现在桩顶; 随着坚向荷载增大, 水平位移最大值和转角最大值将出现在桩中下部; 水平位移和转角随深度先减小至 0 后反向增大, 最后减小至 0; 桩身水平位移受频率影响较大, 管桩中下部转角受频率影响较大。

(4) 坚向荷载使管桩桩身内力发生重分布, 当坚

向荷载为零时, 弯矩最大值出现在桩身中上部, 剪力最大值出现在桩顶; 随着竖向荷载增大, 弯矩最大值和剪力最大值将出现在桩底; 管桩中下部弯矩和剪力受频率影响较大。

(5) 桩长对管桩位移和内力分布规律的影响主要体现在桩身中下部, 桩长取 10, 15 m 时, 位移曲线和内力曲线均出现一次反向弯曲, 桩长取 20, 25 m 时, 位移曲线和内力曲线均出现两次反向弯曲。

(6) 无桩芯土时的桩顶水平位移幅值和转角幅值均明显大于有桩芯土时的桩顶水平位移和转角。

参考文献:

- [1] NOVAK M. Dynamic stiffness and damping of piles[J]. Canadian Geotechnical Journal, 1974, **11**(4): 574 – 598.
- [2] NOVAK M, ABOUL-ELLA F. Impedance functions of piles in layered media[J]. Journal of the Engineering Mechanics Division, 1978, **104**(3): 643 – 661.
- [3] NOVAK M, NOGAMI T. Soil - pile interaction in horizontal vibration[J]. Earthquake Engineering & Structural Dynamics, 1977, **5**(3): 263 – 281.
- [4] NOGAMI T, NOVAK M. Resistance of soil to a horizontally vibrating pile[J]. Earthquake Engineering & Structural Dynamics, 1977, **5**(3): 249 – 261.
- [5] DOYLE P F, PAVLOVIC M N. Vibration of beams on partial elastic foundations[J]. Earthquake Engineering & Structural Dynamics, 1982, **10**(5): 663 – 674.
- [6] EISENBERGER M, YANKELEVSKY D Z, ADIN M A. Vibrations of beams fully or partially supported on elastic foundations[J]. Earthquake Engineering & Structural Dynamics, 1985, **13**(5): 651 – 660.
- [7] GAZETAS G, DOBRY R. Horizontal response of piles in layered soils[J]. Journal of Geotechnical Engineering, ASCE, 1984, **110**(1): 20 – 40.
- [8] 杨军, 宋二祥, 陈肇元. 桩在饱和土中水平振动的辐射阻尼简化算法[J]. 岩土力学, 2002(2): 179 – 183. (YANG Jun, SONG Er-xiang, CHEN Zhao-yuan. Simple radiation damping model for horizontally vibrating pile in saturated soil[J]. Rock and Soil Mechanics, 2002(2): 179 – 183. (in Chinese))
- [9] 尚守平, 余俊, 王海东, 等. 饱和土中桩水平振动分析[J]. 岩土工程学报, 2007, **29**(11): 1696 – 1702. (SHANG Shou-ping, YU Jun, WANG Hai-dong, et al. Horizontal vibration of piles in saturated soil[J]. Chinese Journal of Geotechnical Engineering, 2007, **29**(11): 1696 – 1702. (in Chinese))
- [10] 余俊, 尚守平, 李忠, 等. 饱和土中端承桩水平振动动力响应分析[J]. 岩土工程学报, 2009, **31**(3): 408 – 415. (YU Jun, SHANG Shou-ping, LI Zhong, et al. Dynamical characteristics of an end bearing pile embedded in saturated soil under horizontal vibration[J]. Chinese Journal of Geotechnical Engineering, 2009, **31**(3): 408 – 415. (in Chinese))
- [11] HALABE U B, JAIN S K. Lateral free vibration of a single pile with or without an axial load[J]. Journal of Sound and Vibration, 1996, **195**(3): 531 – 544.
- [12] 周绪红, 蒋建国, 邹银生. 黏弹性介质中考虑轴力作用时桩的动力分析[J]. 土木工程学报, 2005, **38**(2): 87 – 91. (ZHOU Xu-hong, JIANG Jian-guo, ZOU Yin-sheng. Dynamic analysis of piles under axial loading and lateral dynamic force in visco-elastic media[J]. Chinese Civil Engineering Journal, 2005, **38**(2): 87 – 91. (in Chinese))
- [13] CATAL H H. Free vibration of partially supported piles with the effects of bending moment, axial and shear force[J]. Engineering Structures, 2002, **24**(12): 1615 – 1622.
- [14] CATAL H H. Free vibration of semi-rigid connected and partially embedded piles with the effects of the bending moment, axial and shear force[J]. Engineering Structures, 2006, **28**(14): 1911 – 1918.
- [15] LU J F, ZHANG X, WAN J W, et al. The influence of a fixed axial top load on the dynamic response of a single pile[J]. Computers and Geotechnics, 2012, **39**: 54 – 65.
- [16] LIU H L, CHU J, DENG A. Use of large-diameter, cast-in situ concrete pipe piles for embankment over soft clay[J]. Canadian Geotechnical Journal, 2009, **46**(8): 915 – 927.
- [17] LIU H L, NG C W W, FEI K. Performance of a geogrid-reinforced and pile-supported highway embankment over soft clay: case study[J]. Journal of Geotechnical and Geoenvironmental Engineering, 2007, **133**(12): 1483 – 1493.
- [18] XU X T, LIU H L, LEHANE B M. Pipe pile installation effects in soft clay[J]. Geotechnical Engineering, 2006, **159**(4): 285 – 296.
- [19] DING X M, LIU H L, LIU J Y, et al. Wave propagation in a pipe pile for low-strain integrity testing[J]. Journal of Engineering Mechanics, ASCE, 2011, **117**(9): 598 – 609.
- [20] ZHENG C, DING X, LI P, et al. Vertical impedance of an end - bearing pile in viscoelastic soil[J]. International Journal for Numerical and Analytical Methods in Geomechanics, 2014, **39**(6): 676 – 684.
- [21] ZHENG C, LIU H, DING X, et al. Horizontal vibration of a large-diameter pipe pile in viscoelastic soil[J]. Mathematical Problems in Engineering, 2013(3): 1 – 13.